Investigation of Water Clusters Containing OH^- and H_3O^+ Ions in Atmospheric Conditions. A Molecular Dynamics Simulation Study

Elena Brodskaya

Department of Chemistry, St. Petersburg State University, 199034 St. Petersburg, Russia

Alexander P. Lyubartsev and Aatto Laaksonen*

Division of Physical Chemistry, Arrhenius Laboratory, Stockholm University, SE−106 91 Stockholm, Sweden

Received: May 30, 2001; In Final Form: October 16, 2001

Water clusters, formed on the aqueous ions H^+, OH^-, or H_3O^+ are investigated using the molecular dynamics simulation method. Temperature dependence of various cluster properties is studied from 150 to 300 K. The dependence of both the cluster structure and its thermodynamic characteristics on the cluster size (N) is analyzed at 300 K. It is found, based on the energy criteria, that the cluster around the hydronium (H_3O^+) ion is more stable for all cluster sizes, while the work-of-formation criteria predicted the water cluster on the protonated ion to be more stable when $N > 30$. On the bases of work-of-cluster-formation and its size dependent, the nucleation barrier was found to be lower for clusters around hydronium ion than those formed around the hydroxyl ions.

Introduction

Two previous investigations in this series were devoted to studies of local structural, dynamical, electrical. and thermodynamical properties of water clusters formed on a selected set of model metal and halogen ions.[1,2] In this contribution we report results from computer simulations of water clusters containing the three "aqueous" ions: H^+, OH^-, and H_3O^+, called hereafter simply the "water ions". Due to their importance, each one of these three ions alone would deserve an investigation of their own. These ions are common in the Earth's atmosphere where they, to a large extent, give a rise to water condensation, especially at higher altitudes where the physical conditions are characterized by both low temperature and pressure.[3] Also, these ions have a strong influence on phase transitions taking place in small aggregates of water molecules under atmospheric conditions.[4] These water clusters are found to be very stable in mass-spectroscopic experiments[5−9] where the purpose was to measure the enthalpy and the clustering energy.

There are already a great deal of studies reported of water clusters and solutions involving them. However, the main focus in many of these earlier works has been on the proton-transfer mechanism taking place in water.[10−12] Also, construction of H^+−water interaction potentials, taking into account proper quantum mechanical nature of the proton, has been another important problem.[13,14] Among other important issues, there are studies of thermodynamic properties of water clusters with the water ions, including works of phase solid−liquid transition[15] and free energy calculations.[16−18] Particularly the knowledge of free energy or work-of-cluster-formation (W) is important in describing processes connected to water phase transitions.

The main objective in our investigation is to calculate the work-of-cluster-formation and its dependence on the cluster size *W(N),* as well as to study several of other thermodynamic and structural characteristics of water clusters with the three water ions. Compared to previous related papers dealing with thermodynamic properties,[15−18] the use of molecular dynamics (MD) simulation method, allows us to estimate even the kinetic characteristics in the cluster formation.

Computational Details

Models and Methods. All the water clusters contained one ion while the number of water molecules varied within the interval of $10 < N < 100$. The rigid SPC/E potential[19] was used to model the water molecules. Conventional MD simulations were carried out applying the constrained dynamics algorithm.[20] Temperature, varied between 150 and 300 K in different runs, was maintained constant by the Nóse-Hoover thermostat.[21,22] The temperature interval is to correspond to liquid states for all the considered clusters. The time step was chosen equal to 1 fs. Production time to collect the averages was 10 ns or more. No cutoff was applied on the interactions. The ion−water interaction potentials were taken from the literature. For the proton (H^+), the model by Kozak and Jordan,[23] was used but without the polarization effects. We are aware that omission of polarization effects is a crude approximation but we believe that it should not change the main conclusions at the end. The rigid pyramidal model by Fornili et al.[24] was chosen for the hydronium (H_3O^+) ion. Two hydroxide ion (OH^-) models were used. The first (model 1) is the rigid model by Andoloro et al.[25] The second model (model 2) was constructed from the SPC/E model by simply removing one hydrogen and setting the charge $-1.4238|e|$ on the oxygen atom. We can therefore describe this instant model, as "a deprotonated SPC/E water" or "SPC/E hydroxide ion". Both ion potentials, the one reported by Fornili et. al.[24] and the potential introduced by Andoloro et al.,[25] are constructed by fitting the dimer data from ab initio quantum chemical calculations to an analytical expression.

Model 2 for the hydroxide ion is a pure ad hoc construction. It is introduced in attempt to reproduce the basic features of the OH^- ion in SPC/E water. Another reason for proposing it was the obvious inability of model 1 to reproduce the energies

10.1021/jp012053o CCC: $22.00
Published on Web 05/25/2002

of water clusters. There are a few hydroxide models,[17,18] but they are rather difficult to implement in molecular dynamics simulations. Despite its ad hoc character, model 2 reproduces reasonably well the experimental energies of water clusters.

The initial configurations were taken from our previous simulations[1,2] of corresponding clusters with a cation or an anion of a comparable size in the center of the cluster. After replacing the original ion with one of the water ions, the system was cooled to $T = 150$ K and the simulation was started. Since we are interested in the liquid state of the clusters, this choice of the initial state should be quite appropriate. The aqueous ions are free to move inside the cluster together with water molecules.

Analysis Tools. The local internal structure of the clusters can be characterized by a number of different radial profiles and correlation functions. For example, the calculated local particle density $\rho_i(r)$ of the ion "*i*" describes its averaged distribution in the cluster. Similarly the local density of the water molecules in the cluster is given by $\rho_w(r)$. A radial profile, for an effectively spherical cluster, describes the dependence of the studied local quantity as a function of the distance from the center of mass of the system. In addition to the radial profiles of the atomic densities $\rho_i(r)$ and $\rho_w(r)$, the total $e(r)$ and kinetic $e_k(r)$ energies per particle, the electric polarization vector, and the local electric potential $\varphi(r)$ and the normal pressure $P_N(r)$ have also been calculated. In the calculations of the partial local energy, separately for the ion ($e_i(r)$) and water ($e_w(r)$), their interaction energy has been equally divided between them.

The arrangement of water molecules with respect to the charged ion was described by three orientational distribution functions $\rho(\vartheta)$, constructed from the dipole moment vector, or from the HH or OH vectors of the water molecules.

The electric potential $\varphi(r)$ was calculated on the basis of following equation:

$$\varphi(r) = \frac{1}{4\pi\epsilon_0}\left\langle \sum_{r_i<r} \frac{q_i}{r} + \sum_{r_i>r} \frac{q_i}{r_i} \right\rangle$$

The parameter q_i is the atomic (or ionic) charge and r_i its distance from the center-of-mass of the system. The brackets denote the time average.

The cluster as a whole can be characterized by its total energy E, the energy contributions from the water−water U_{ww}, and ion−water U_{wi} interaction, and by the work-of-cluster-formation W. The work-of-cluster-formation on an ion W was obtained by integrating the total normal pressure $P_N(r)$ according to

$$W = 2\pi \int_0^{R_\beta} P_N(r) r^2 \, dr - 2\pi P^\beta R_\beta{}^3/3$$

P^β and R_β are the pressure of vapor and the radius of the sphere located inside the vapor range, respectively.

The dynamical behavior of the molecules in the clusters is described by the diffusion coefficients. Both D_w (water) and D_i (ions) are calculated from the time dependence of the mean square displacement according to the Einstein relationship.

Results and Discussion

Local Properties. *Clusters with H^+.* A snapshot of a cluster consisting of 20 water molecules and one proton at 300 K is shown in Figure 1. The proton is tightly coordinated to one of the water molecules to form a H_3O^+ complex. Some related average local characteristics for the system shown in Figure 1 are given in Figure 2, such as the local density and local energy for water and the proton, are at the two temperatures (150 and

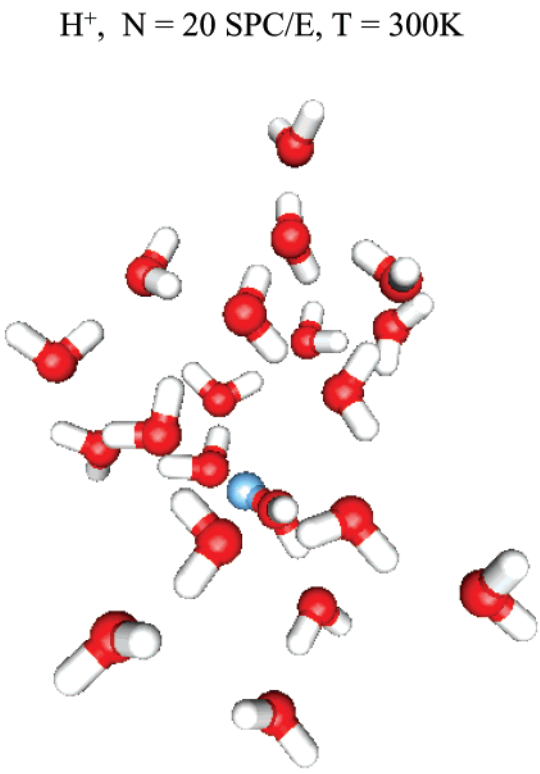

Figure 1. Snapshot of the configuration in the cluster with $N = 20$ SPC/E water molecules and H^+ at 300 K.

300 K). It can be seen from the radial density profile at 150 K (Figure 2a) that the most probable position of the proton is shifted about 2 Å from the center of the cluster (its initial position). A similar shift of the most probable position of the proton (1 Å at 150 K and 2 Å at 180 K, respectively), was observed even in ref 15, where the polarizable model by Kozak and Jordan[23] was used. At 300 K the proton can be found practically everywhere in the cluster with an equal probability. The local ion energy (Figure 2b) is characterized by a deep minimum shifted to 2.5 Å from the center of mass of the cluster. The depth of the minimum decreases slightly after heating the system from 150 to 300 K at the same time as the distribution of the local ion energy becomes wider and more flat. As a result of using different water−water and ion−water potentials, the energy of the proton-containing cluster with 20 SPC/E water molecules was about 10% higher in our calculations than it was reported in ref 15.

The peak of the ion−oxygen pair-correlation function (Figure 2c) is located at about 1 Å. The integrated coordination number around the proton is about 2.2 and seems rather independent of the temperature, meaning that the $H_5O_2^+$ complex should be dominating in this system.

Based on the overall water density it is possible to conclude that the cluster is in a liquid state even at 150 K, although some elements of order already appear. At the higher temperature, 300 K, the water density profile is similar to that obtained for the pure water cluster, indicating that the proton does not perturb the water structure in the region of its liquidlike state.

Clusters with H_3O^+. The simulations of water clusters with the proton dissolved in water showed that H^+ is most of the time trapped in a complex with one or two water molecules. From the experiment it is established that the former, the H_3O^+ complex, is quite long living. Therefore it is reasonable to consider the H_3O^+ complex as an ion, commonly known as the hydronium ion. In fact, it should be kept in mind that the clusters

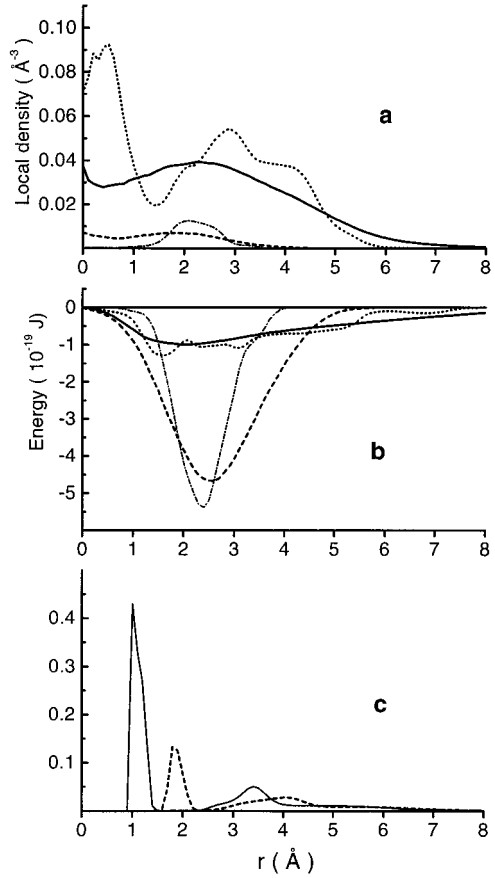

Figure 2. (a) The radial profiles of the local density (in A^{-3}) and (b) energy per particle (in 10^{-19}J) at 150 K (water, dotted line; ion, dashed−dotted line) and 300 K (water, solid line; ion, dashed line). (c) The water−ion correlation functions (O_wH_i, solid line; H_wH_i, dashed line) at 300 K in the cluster with $N = 20$ SPC/E water molecules and H^+.

containing H^+ and H_3O^+ should be seen as two models of the "real" positively charged water clusters. We have taken the rigid model for this ion with a pyramidal geometry and its charge uniformly distributed among three protons from the work by Fornili et al.[24]

An instantaneous snapshot of the cluster with 20 water molecules and one hydronium ion at 150 and 300 K are shown in Figure 3. The ion is found close to the center of the cluster at both temperatures. At 150 K some directional order can be observed around the ion. At this temperature a general overall feature is a branch-like structure of the cluster with three groups of water molecules developing in the directions of three hydrogen atoms of the hydronium ion, rather than a clathrate-like structure. The clathrate-like structure has received some considerable support in the literature,[8] but also disputed recently.[26] It may also be possible that we did not obtain the clathrate structure because we simulated the system at 150 K by starting from an initial configuration taken from a simulation carried out at a higher temperature. A branched water-cluster structure around the hydronium ion was also observed in ref 16, where the polarizable model by Kozak and Jordan[27] was applied. At the first sight this seems to be like the edge-shared prismic structure as it was proposed in ref 26. When the temperature is increased the cluster structure becomes slightly randomized. Still, even at 300 K, the water molecules do not approach the hydronium ion from its oxygen side**.** At the oxygen side of the hydronium ion**,** the water molecules appear only in the second hydration shell of the ion. The hydronium ion has almost all the time typically three water molecules in the first

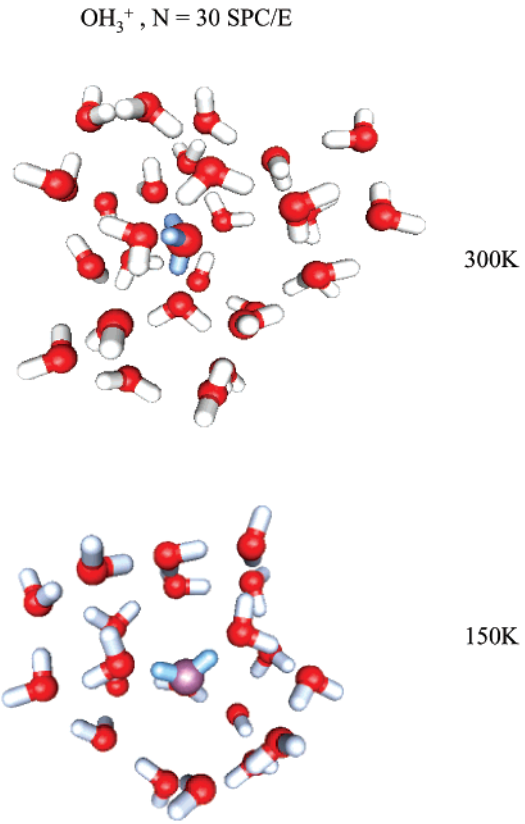

Figure 3. Snapshot of the configuration in the cluster with H_3O^+ and $N = 20$ SPC/E water molecules at (a) 150 and (b) $N = 30$ at 300 K.

hydration shell with their oxygen atoms directed toward the hydronium protons.

This can also be confirmed by analyzing the pair distribution functions (Figure 4c). Calculated from the oxygen−oxygen correlation function, the coordination number of the hydronium in a cluster with 20 water molecules at $T = 300$ K is equal to 3 rather than 4, found for the same ion in the bulk water.[24] This effect can be caused by the limited number of water molecules together with their more loose structure in the cluster. Naturally, the use of different water models in our simulations, and those employed in ref 24 may play a certain role. It should be mentioned that the hydration number 3 for the hydronium ion agrees well with the data from ab initio simulations of liquid water, reported by Tuckerman et al. in ref 14 and with the simulation results after taking into account three-body forces.[28] It should be mentioned that the potential of Fornili et al. does not give 4 as the coordination number in the bulk.[24] Our results agree with those reported in ref 28 in the sense that the first hydration shell is well separated from the second shell. Another different value of the hydration number, slightly above 2, was reported in ref 17. It was obtained with a new interaction potential proposed in that paper. Note also that in our work the closest distance between the H_3O^+ ion proton and the water oxygen is about 1.25 Å (Figure 4c).

The radial profiles of the atomic density and the total energy per particle for the clusters with 20 water molecules at different temperatures are shown in Figure 4. The hydronium ion occupies mostly the center of the cluster independently on the temperature. By looking at the different water density profiles (Figure 4a) one can see how the local density changes with 50 K increments from 150 to 300 K. It is obvious that the cluster appears as a liquid at $T \geq 200$ K. A significant change in the profile is, however, observed at 150 K where two well-separated

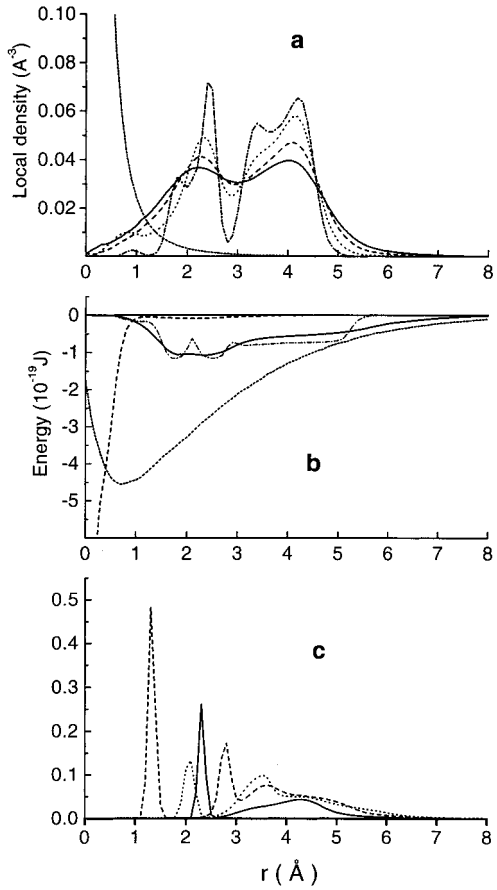

Figure 4. (a) The radial profiles of the local density (in A^{-3}) and (b) energy per particle (in 10^{-19}J) at the different temperatures (water at 300 K, solid line; water at 250 K, dashed line; water at 200 K, dotted line; water at 150 K, dash−dotted line; ion at 300 K, short dashed line). (c) The water−ion correlation functions (O_wO_i, solid line; O_wH_i, dashed line; H_wH_i, dotted line) at 300 K in the cluster with $N = 20$ SPC/E water molecules and H_3O^+.

hydration shells appear around the center occupied by the hydronium ion. This may probably be related to a frozen state, although we cannot say this definitely without a more detailed analysis of the behavior of the water molecules. To investigate it closer is one of our future objectives. Nevertheless, as will be shown below, the diffusion coefficient in this system is very small for both water and the ion at 150 K.

Comparison of the water density profiles in Figures 2 and 4 allows one to conclude that the cluster with the hydronium ion shows a somewhat more compact structure than is the case with the proton. The more loose cluster structure around the proton is a consequence of its larger mobility, although it is not possible to describe the proton mobility accurately within this purely classical model.

The contribution to the energy from the ion−water interactions appears to be of same order of magnitude within the considered models for both the proton and hydronium ions. They both have the same depth of the local energy minimum for $e_i(r)$ (see Figure 4b**)**.

Clusters with OH$^-$. Studies of the negative hydroxyl ion (hydroxide) are much less frequent in the literature than those dealing with the two positive water ions, discussed above. The experiments show that the clusters with the OH^- ion are less stable than the clusters around the positive protonated ions,[9] but nevertheless, they are still fairly long-living aggregates. Simulations of such clusters have been carried out in refs 18 and 29 using the Monte Carlo method. The largest cluster

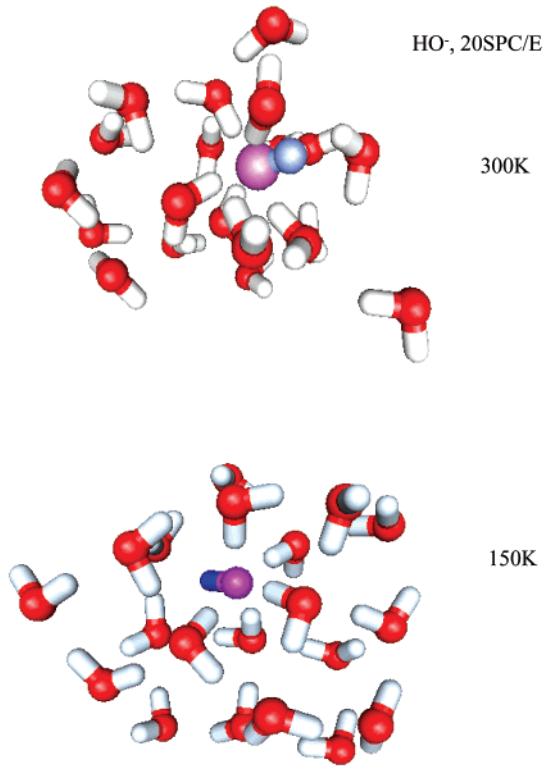

Figure 5. Snapshot of the configuration in the cluster with HO^- and $N = 20$ SPC/E water molecules at (a) 150 K and (b) 300 K.

studied in ref 29 had five water molecules. Here our aim is to extend the cluster sizes considerably beyond that.

In the simulations, two different models were used for the hydroxyl ion; one taken from the work by Andaloro et al.[25] (model 1), while the other was constructed as the deprotonated ion of the SPC/E water molecule with the excess negative charge (corresponding to that of one electron) added on the oxygen, called below as model 2. The model 1 is characterized by its substantially stronger interactions, resulting in more compact clusters compared to those formed around the SPC/E-like hydroxide.

Again, typical snapshots of molecular configurations in clusters with 20 water molecules with the hydroxyl ion (model 2) at 150 and 300 K are shown in Figure 5. It can be seen that the OH^- ion has moved from the center of cluster with its only proton directed outward of the cluster. In the close vicinity of the negatively charged hydroxyl oxygen there are approximately six water molecules. This picture does not change much after increasing the temperature, except that the positions of water molecules in the second hydration shell become slightly more randomized at 300 K compared to how they are located at 150 K. The difference between the two models is not obvious from the snapshots but becomes more clear from the radial profiles of the local characteristics, shown in Figures 6 and 7. At 150 K, the hydroxyl is found close to the center-of-mass of the cluster for the both models with the water molecules being expelled from this region. Compared to model 1, the water distribution of model 2 (Figure 6a) shows somewhat more order with two developed hydration shells (Figure 7a). The situation is, however, changed when the temperature is increased to 300 K. In the case of model 2, both the hydroxyl ion and water molecules move freely in the cluster. The ion density shows a wide maximum at the cluster center and the water distribution becomes similar to that found for the pure water cluster (Figure 6a). However, for model 1 there is no substantial change in the

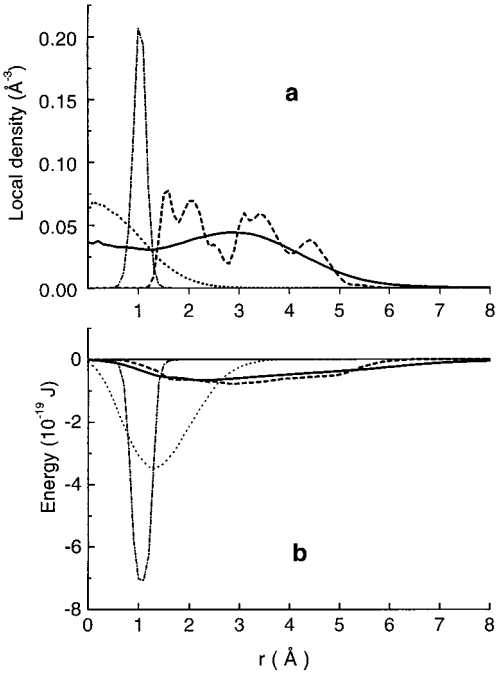

Figure 6. (a) The radial profiles of the local density (in A^{-3}) and (b) energy per particle (in 10^{-19}J) at 150 K (water, dashed line; ion, dashed−dotted line) and 300 K (water, solid line; ion, dotted line) in the cluster with $N = 20$ SPC/E water molecules and HO^- (model 2).

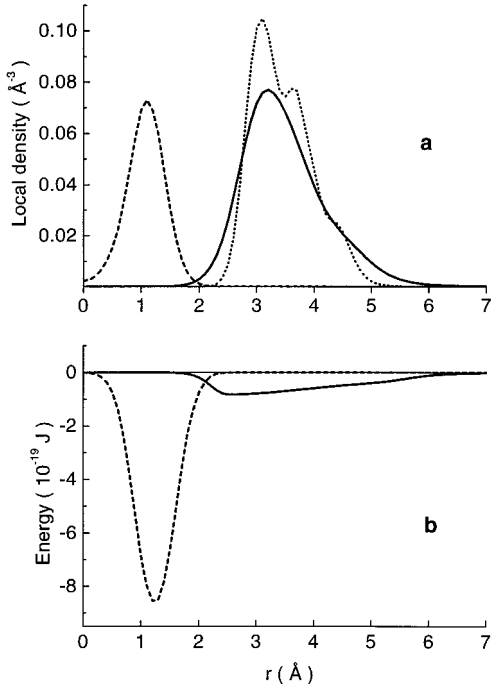

Figure 7. (a) The radial profiles of the local density (in A^{-3}) at 150 K (water, dotted line) and 300 K (water, solid line; ion, dashed line) and (b) energy per particle (in 10^{-19}J) at 300 K (water, solid line; ion, dashed line) in the cluster with $N = 20$ SPC/E water molecules and HO^- (model 1).

ion and water distribution after increasing the temperature (Figure 7a). There are two clearly visible distinct regions, one around the cluster center occupied by the ion, and the other region near the cluster surface occupied by water molecules.

The pair correlation functions between the hydroxyl oxygen, and O and H atoms of water, respectively ($g_{O_iO_w}$ and $g_{O_iH_w}$) are similar for the both models (Figures 8 and 9), although their integrated coordination numbers differ. The first coordination number for the Andaloro model is equal to 6.8 (to be compared

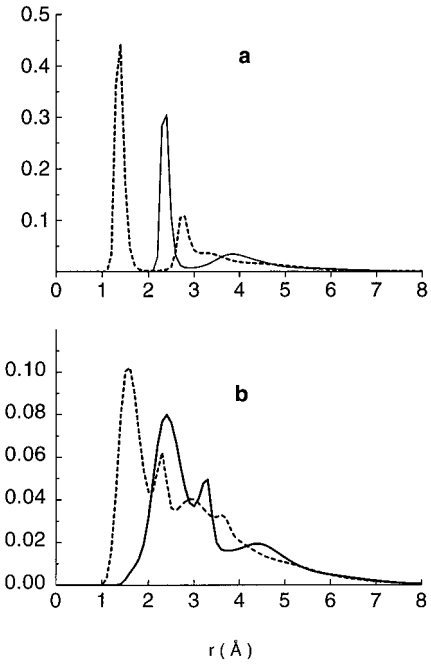

Figure 8. The ion−water correlation functions: (a) $g_{O_iO_w}(r)$ (solid line) and $g_{O_iH_w}(r)$ (dashed line) and (b) $g_{H_iO_w}(r)$ (solid line) and $g_{H_iH_w}(r)$ (dashed line) at 300 K in the cluster with $N = 20$ SPC/E water molecules and HO^- (model 2).

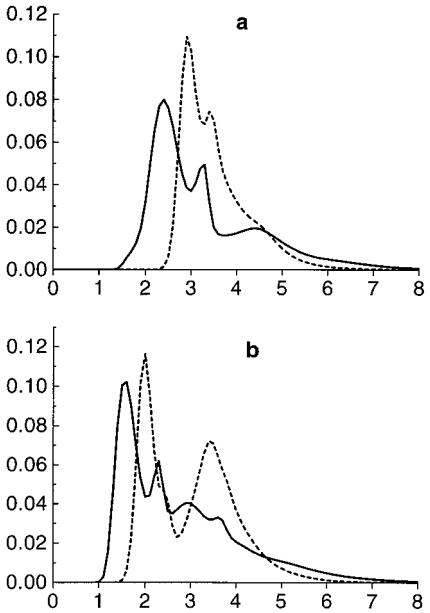

Figure 9. The ion−water correlation functions: (a) $g_{H_iO_w}(r)$ and (b) $g_{H_iH_w}(r)$ for two models of HO^- (model 1, dashed line; model 2, solid line) in the cluster with $N = 20$ SPC/E water molecules HO^-.

to 5 for bulk water).[25] In the case of the SPC/E-like hydroxide this number is equal to 6, which agrees well with the quantum mechanical results reported in ref 14. The position of the first peak of the oxygen−oxygen function for model 2 is shifted slightly toward the ion-oxygen. Based on the peak positions of the oxygen−oxygen and oxygen−hydrogen ion−water correlation functions in model 2, one can see that the hydrogen bond $O_i^-\cdots H-O_w$, between the ion oxygen and H−O covalent bond of the water molecule is linear. Somewhat more significant difference between the two models can be observed in the pair correlation functions for the hydroxyl hydrogen and water atoms ($g_{H_iO_w}$ and $g_{H_iH_w}$) (Figure 9). The distances between the hydroxyl

TABLE 1: Average Properties of Water Cluster with $N = 20$ SPC/E and Ions

ion	T/K	$-e^a$/ 10^{-19} J/molecule	$-u_{ww}{}^b$/ 10^{-19} J/molecule	$-u_{iw}{}^c$/ 10^{-19} J/molecule	$W^d/10^{-19}$ J	$W_0{}^e/10^{-19}$ J	$D_w{}^f/10^{-5}$ cm^2 s^{-1}	$D_i{}^g/10^{-5}$ cm^2 s^{-1}
H^+	150	1.277	0.467	0.872	0.31	3.64	0.03	0.01
H_3O^+		1.200	0.520	0.745	−1.78	2.63	0.017	0.003
HO^- (1)		1.343	0.338	1.068	−5.27	1.74	0.009	0.001
HO^- (2)		1.048	0.381	0.730	−3.65	3.50		
H^+	200	1.203	0.415	0.874	1.66	5.18	0.50	0.12
H_3O^+		1.140	0.483	0.740	−2.12	2.53	0.19	0.02
HO^- (1)		1.282	0.309	1.058	−5.09	2.07	0.12	0.02
HO^- (2)		0.975	0.355	0.714	−3.48	3.19	0.24	0.03
H^+	250	1.130	0.358	0.878	2.24	5.87	1.3	0.5
H_3O^+		1.067	0.440	0.731	−1.78	2.71	0.83	0.06
HO^- (1)		1.217	0.282	1.038	−4.89	2.26	0.56	0.08
HO^- (2)		0.905	0.326	0.686	−3.04	3.28	1.1	0.16
H^+	300	1.062	0.309	0.880	2.36	6.04	1.4	0.70
H_3O^+		0.993	0.394	0.723	−1.55	2.75	1.3	0.08
HO^- (1)		1.144	0.250	1.018	−4.68	2.43	1.1	0.11
HO^- (2)		0.830	0.285	0.675	−2.60	3.10	2.3	0.36

[a] Total energy of cluster per molecule. [b] Potential energy of water−water interaction per molecule. [c] Potential energy of ion−water interaction per molecule. [d] Work of cluster formation. [e] Contribution to work of cluster formation from water−water interaction. [f] Diffusion coefficienf for water. [g] Diffusion coefficienf for the ion.

hydrogen and the water atoms are about 0.5 Å longer in the case of model 1 compared to model 2.

Overall Properties of $N = 20$ Clusters. The total energy per particle e and the contribution from the water−water u_{ww} and ion−water u_{iw} interactions per molecule for clusters with 20 water molecules are given in Table 1 at different temperatures. This table also quotes the values of the work-of-cluster-formation W, the pure water contribution to the work W_0, and the diffusion coefficients both for water D_w and ions D_i. We can see that the values of e and W for model 1 of the hydroxyl ion are even lower than those for the hydronium ion (H_3O^+), corresponding to a more stable state for the clusters with the hydroxyl ion. This is in contradiction with the experimental results.[8,9] Concerning the relative energies between the hydroxyl and hydronium ions, the situation seems better using the model 2.

It should be commented that it is not possible to conclude, whether water condensates easier around hydronium or hydroxyl ion from the difference between the W values for the clusters with hydroxyl and hydronium ions. The obtained results do not allow us to estimate the barrier for the water condensation, which is the difference of W for the two equilibrium states of the system, one corresponding to stable equilibrium of the solvated ion while the other is an unstable equilibrium related to a larger critical nucleus. Unfortunately it is not possible to solve this important problem without varying the cluster size. We shall return to this question later when the dependence of cluster properties will be discussed as a function of the cluster size. It should also be mentioned that our calculations deal with the reversible work for the equilibrated clusters whereas we do not know the chemical potential of the system.

It can be seen from Table 1 that the absolute contribution from the ion−water interaction is about twice as large as that from the water−water interactions. This contribution is also less temperature-dependent than the water−water interactions, which are weakening substantially with increasing the system temperature. As a consequence of this, the absolute value of the total energy will decrease with the increasing temperature.

The work-of-cluster-formation with both the hydronium and hydroxyl ions behaves quite similarly to that obtained previously for the clusters with the alkali ions.[1,2] The total work is negative, according to the preference of water to condensate on the ion. The work-of-cluster-formation with the proton however has opposite (positive) sign than the work-of-cluster-formation for the other ions. Therefore, based on the work-of-formation, obtained with the present models, the cluster formed on the hydronium ion should be more stable than the one formed on an isolated proton. This can be expected from the behavior of the proton and its involvement in the complex formation with water molecules. The simplest of these complexes is the one formed with the hydronium ion.

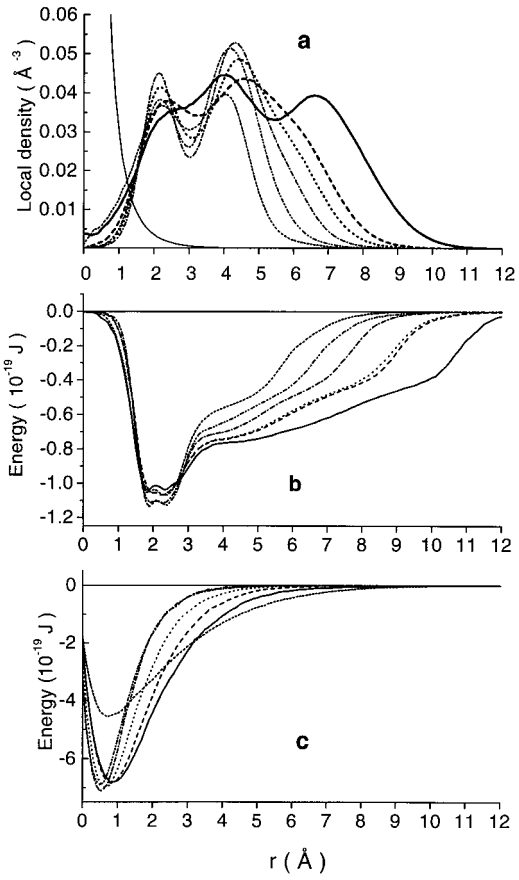

Figure 10. (a) The radial profiles of the local density (in A^{-3}) for ion (thin solid curve) and water (six curves); (b) energy per particle (in 10^{-19}J) for water and (c) ion at 300 K in the cluster with a different number of water molecules and one H_3O^+. $N = 100$ (solid line both for water and ion), 60 (dashed line), 50 (dotted line), 40 (dashed−dotted line), 30 (dash−dot-dotted line), 20 (short dashed line).

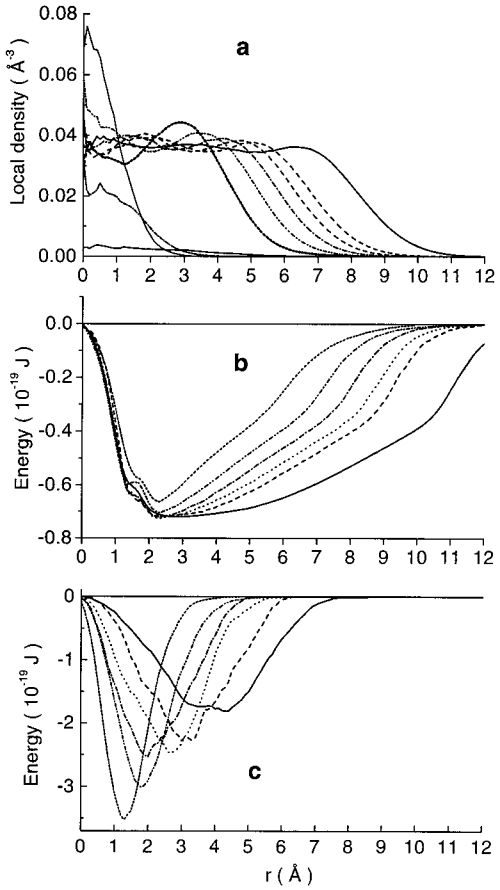

Figure 11. (a) The radial profiles of the local density (in A^{-3}); (b) energy per particle (in 10^{-19}J) for water and (c) ion at 300 K in the cluster with a different number of water molecules and one HO^-. $N =$ 100 (solid line both for water and ion), 60 (dashed line), 50 (dotted line), 40 (dashed−dotted line), 30 (dash−dot−dotted line for water density and short dashed−dotted for ion density), 20 (short dashed line for water density and short dot for ion density).

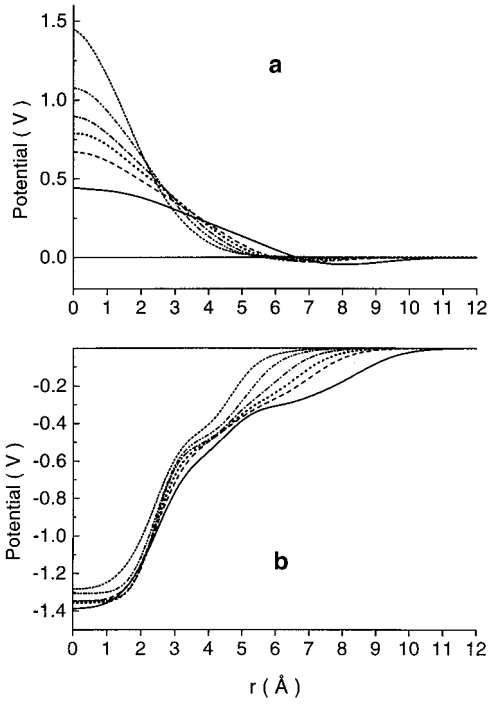

Figure 12. The radial profiles of the water contribution to the local electric potential (in V) in the cluster with the different number of water molecules and (a) one HO^- or one (b) H_3O^+ at 300 K. $N = 100$ (solid line), 60 (dashed line), 50 (dotted line), 40 (dash−dotted line), 30 (dash−dot−dotted line), 20 (short dashed line).

The work-of-cluster-formation increases with the temperature more strongly in the systems with the negative hydroxyl ion. Compared to hydronium ion the hydroxyl ion is also more mobile at higher temperatures according to its larger diffusion coefficient D_i. Also, the water mobility is higher in the clusters with the hydroxyl ion (model 2) compared to that obtained with the hydronium ion. The very low diffusion coefficients, both for water and the ion in the cluster with the hydronium ion at 150 K correspond most likely to a solid state of this system, as it was mentioned above. Generally, the water diffusion coefficients are lower in the clusters with the aqueous ions than those in bulk water. This is generally true for alkali ions, however, in the case of water clusters with the potassium ion, it was found to be the other way around.[1]

Dependence of the Cluster Properties on the Cluster Size. According to Table 1, the work-of-formation for the cluster with the hydroxyl ion is less than that with the hydronium for the clusters consisting of 20 water molecules. This result is in disagreement with the experimental prediction that protonated water ions would give more stable clusters.[8,9] In this context it may be useful to investigate how the cluster properties depend on the cluster size. Simulations of clusters with the number of water molecules N varying from 10 to 100 have therefore been undertaken at 300 K.

The radial profiles of the local density and total energy for both water and the ion in clusters are shown in Figures 10 and 11. The hydronium ion is found mainly in the vicinity of the cluster center independently on the cluster size. For hydroxyl ion the behavior is quite different. We can see that larger grows the cluster, wider becomes the distribution of hydroxyl ions relative to the cluster center-of-mass. In the case of the cluster with 100 water molecules, the distribution has become practically uniform (Figure 11a).

The water distribution in the clusters with the hydronium ion is more structured compared to the smooth water distribution in the corresponding clusters with the hydroxyl. For example, it is possible to see two water shells in the clusters formed around the hydronium ion in the case of $N < 100$ (Figure 10a), while such shell structure has disappeared for $N = 100$. It is also interesting to see that the minimum between the shells changes nonmonotonically with N. It reaches its lowest value for $N = 40$ and for a cluster of this size the energy per particle also approaches the lowest value both for the waters and the ion. In the case of the hydroxyl ion the values of these minima are decreasing monotonically with N.

The water contribution to the local electric potential $\varphi(r)$ is shown in Figure 12. Similarly to the local energy (Figures 10b and 11b), there is no region in the cluster with a constant (not even nearly) value of the electric potential. The potential is negative for the clusters with hydronium ion, and it becomes more negative with an increase of the cluster size. The main features of this function are similar to that obtained for the pure water cluster except that it is more negative in a charged cluster. It means most likely that the internal structure of the clusters with the hydronium should be similar to that of the pure water clusters. The changes with N found in the local potential in the clusters containing the hydroxyl are somewhat peculiar. The positive values of $\varphi(r)$ in the central region of the cluster are decreasing and the function changes its sign in the surface layer and becomes negative. Such behavior can be understood by keeping in mind that the potential is determined by the local distribution of the atomic charges of water molecules, leading

TABLE 2: Dependence of the Work of Cluster Formation and the Diffusion Coefficient on the Number of Molecules *N* in Clusters at 300 K in Water Clusters with H_3O^+ Ion and Hydroxyl Ion

ion	N	$W^a/10^{-19}$ J	$W_0{}^b/10^{-19}$ J	$D_w{}^c/10^{-5}$ cm^2 s^{-1}	$D_i{}^d/10^{-5}$ cm^2 s^{-1}
			(a) H_3O^+ Ion		
H_3O^+	10	−0.51	2.15	0.7	0.17
H_3O^+	20	−1.55	2.75	1.3	0.07
H_3O^+	30	−2.55	3.43	1.5	0.02
H_3O^+	40	−2.96	4.05	1.6	0.004
H_3O^+	50	−3.00	4.63	1.7	0.03
H_3O^+	60	−2.83	5.23	1.9	0.03
H_3O^+	100	−2.38	7.32	2.2	0.06
			(b) Hydroxyl Ion		
HO^-	10	−3.04	2.66	2.3	0.16
HO^-	20	−2.60	3.10	2.3	0.36
HO^-	30	−1.92	3.87	2.5	0.5
HO^-	40	−1.35	4.30	2.7	0.6
HO^-	50	−0.88	4.73	2.8	0.6
HO^-	60	−0.52	5.11	2.9	0.7
HO^-	100	0.72	6.47	3.0	0.7

[a] Work of cluster formation. [b] Contribution from water−water interaction. [c] Diffusion coefficienf for water. [d] Diffusion coefficienf for the ion.

to a negative value of the electrostatic potential in pure water clusters.[30] In clusters with ions, the ion field affects the orientations of the water molecules. However, at large distances from the ion, this perturbation becomes weaker. As a result of this, the electrostatic potential from the water molecules becomes more negative in the field of a positive ion while in the field of a negative ion it is positive. In bigger clusters this effect due the ion is not strong enough to reorient the water molecules in the surface region. That is why the electrostatic potential becomes negative in the both cases, as it is in the case of pure water. For example, this effect can be observed for a cluster of $N = 100$ water molecules around a OH^- ion.(Figure 12a)

The mobility of the hydroxyl ion is found almost 1 order of magnitude higher than that of the hydronium ion, according to the data of Table 2, where diffusion coefficients of ion D_i and water D_w are listed. The diffusion coefficient of water is larger in the clusters with the hydroxyl ion. In both systems D_w increases slightly with *N*. This increase is due to the increasing contributions from the molecules in the surface layer.

The average value of the total energy *E*, the contribution from the water−water U_{ww} and ion−water U_{iw} interactions, and their values per particle (*e*, u_{ww}, and u_{iw}) are given in Table 3 for the hydronium ion (a) and hydroxyl ion (b). As it was already

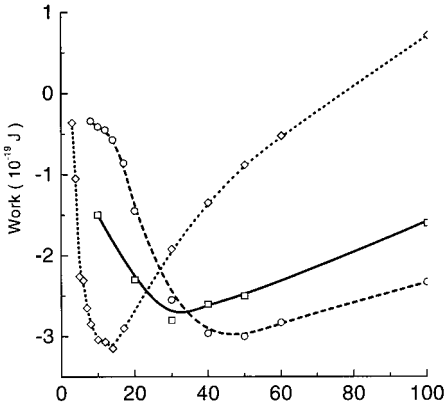

Figure 13. The dependence of the work of cluster formation (in 10^{-19}J) with K^+ (solid line), H_3O^+ (dashed line) and HO^- (model 2, dotted line) on the cluster size at 300 K.

observed for the cluster with 20 molecules, all energetic characteristics in all the clusters with the hydronium ion are lower than those in the clusters with the hydroxyl ion. For the intensive quantities *e*, u_{ww}, and u_{iw}, the difference for both ions becomes less as *N* increases. The absolute values of the corresponding extensive energies (*E*, U_{ww}, and U_{iw}) increase with *N* in systems with all the ions. So does even the intensive contribution u_{ww} from the water−water interactions. However the absolute values of *e* and u_{iw} decrease with the increase of *N*. Since the intensive contributions u_{ww} and u_{iw} to the total energy *e* are changed differently with *N*, the dependence of the intensive total energy on *N* may not be monotonic within a wider range of the cluster size. This was also observed earlier in the clusters with the potassium ion[2]. It should be noted that for the hydronium ion the clustering energy, describing the change of the energy with the cluster size, is in a good agreement with the experimental data[6] for $10 < N < 30$, where this quantity changes only slightly. The estimated average value from the simulations is about −10.5 kcal/mol for the hydronium ion and about −9 kcal/mol for the hydroxyl ion.

The work-of-cluster-formation *W* was evaluated using eq 2, based on the local normal pressure $P_N(r)$. The values of *W* together with the contribution from the water−water interaction W_0 are listed in Table 2 for the hydronium ion (a) and the hydroxyl ion (b). The dependence of *W* on the cluster size is also shown in Figure 13. The minimum of this function is a result of the competition between two contributions, one from the presence of the ion and the other due to the surface of the system. Again, the dependence of work-of-cluster-formation of

TABLE 3: Dependence of the Energy Characteristics of Water Clusters with H_3O^+ Ion and Hydroxyl Ion on the Number of Molecules *N* in Clusters at 300 K

ion	N	$-E^a/10^{-19}$ J	$-U_{ww}{}^b/10^{-19}$ J	$-U_{iw}{}^c/10^{-19}$ J	$-e^d/10^{-19}$ J/molecule	$-u_{ww}{}^e/10^{-19}$ J/molecule	$-u_{iw}{}^f/10^{-19}$ J/molecule
H_3O^+	10	12.41	1.55	12.22	1.241	0.155	1.222
H_3O^+	20	19.73	7.88	14.46	0.987	0.394	0.723
H_3O^+	30	27.37	14.88	16.34	0.912	0.496	0.545
H_3O^+	40	34.32	22.10	17.32	0.858	0.553	0.433
H_3O^+	50	41.03	29.36	18.06	0.821	0.587	0.361
H_3O^+	60	47.65	45.91	18.64	0.794	0.765	0.311
H_3O^+	100	74.19	66.43	20.05	0.742	0.664	0.200
HO^-	10	10.46	−0.26	12.07	1.046	−0.026	1.207
HO^-	20	16.61	5.69	13.50	0.831	0.285	0.675
HO^-	30	22.75	12.60	13.98	0.758	0.420	0.466
HO^-	40	28.93	19.77	14.24	0.723	0.494	0.356
HO^-	50	35.16	27.02	14.46	0.703	0.540	0.289
HO^-	60	41.39	34.31	14.64	0.690	0.572	0.244
HO^-	100	66.60	64.75	15.37	0.666	0.648	0.154

[a] Total energy of cluster. [b] Potential energy of water−water interaction. [c] Potential energy of ion−water interaction. [d] This energy of cluster per molecule. [e] This energy per molecule. [f] This energy per molecule.

the hydronium ion on the cluster size is similar to what was obtained for the clusters containing potassium ion.[2] In the case of the hydroxyl ion, the minimum is found among the smaller clusters. For the SPC/E water model the most stable clusters at 300 K should be expected to have about 17 molecules with the hydroxyl ion and about 40 with the hydronium ion. It is interesting to notice that the minimum of the work of cluster formation with the hydronium ion is reached in the interval $40 < N < 50$ where the extreme values of the local energy are observed (Figure 10b,c). Also the clusters within this range are characterized by the most developed shell structure (Figure 10a).

The observed correlation in the size dependence of the work-of-cluster-formation with the hydronium and hydroxyl ions (see Figure 13) allows us to suggest that the barrier against the nucleation would be lower in the case of the hydronium ion in comparison with the hydroxyl ion. It means that larger water aggregates should preferably be formed around the hydronium ion.

Conclusions

On the bases of our MD simulation results, we can formulate following conclusions, both for water and the water ions. We should, of course, keep in mind that all these simulations are carried out using rigid potential models.

- Classical MD (thus neglecting the phenomenon of proton transfer) can describe reasonably well the thermodynamic properties of water clusters condensed on the hydroxyl and protonated.
- The small protonated clusters show a clear hydration shell structure, which becomes gradually destroyed when the number of molecule reaches approximately 100.
- The clusters with the hydronium ion are characterized by lower values of the energy compared to the clusters of the same size formed with the hydroxyl ion.
- According to the local electric potential, the hydronium ion perturbs less the internal water structure in the clusters compared to that of the hydroxyl ion.
- The correlation of the size dependence of the work-of-cluster-formation shows that the barrier against the nucleation should be lower in the case of the hydronium ion compared to the hydroxyl ion.

Acknowledgment. This work has been supported by NFR (The Swedish Natural Science Research Council) by research grants to A.L. and visiting professorship to E.B. E.B. also gratefully acknowledges the grants of Russian Foundation for Basic Research (Grants 00-15-97357 and 01-03-32334).

References and Notes

(1) Brodskaya, E. N.; Lyubartsev, A. P.; Laaksonen, A. *J. Chem. Phys.* **2002**, *116*, 7879.
(2) Egorov, A. V.; Brodskaya, E. N.; Laaksonen, A. *Mol. Phys.* **2002**, *100*, 941.
(3) Wayne, R. P. *Chemistry of Atmosphere*; Oxford: University Press. 2000.
(4) Seinfeld, J. H.; Pandis, S. N. A*tmospheric Chemistry and Physics: From Air Pollution to Climate Change*; Wiley: New York, 1998.
(5) Kebarle, P.; Searles, S. K.; Zolla, A.; Scarborough, J.; Arshadi, M. *J. Am. Chem. Soc*. **1967**, *89*, 6393.
(6) Arshadi, M.; Kebarle, P. *J. Phys. Chem*. **1970**, *74*, 1483.
(7) Mautner M.; Speller C. V. *J. Phys. Chem.* **1986**, *90*, 6616.
(8) Shi, Z.; Ford, J. V.; Wei, S.; Castleman, A. W., Jr. *J. Chem. Phys.* **1991**, *94*, 268; *J. Chem. Phys*. **1993**, *99*, 8009.
(9) Yang, X.; Castleman, A. W., Jr. *J. Phys. Chem*. **1990**, *94*, 8500.
(10) Lobaugh, J.; Voth, G. A. *J. Chem. Phys*. **2000**, *104*, 2056.
(11) David, C. W. *J. Chem. Phys*. **1996**, *104*, 7255.
(12) Vuilleumier, R.; Borgis, D. *J. Chem. Phys*. **1999**, *111*, 4251. *J. Mol. Struct*. **1997**, *436*−*437*, 555.
(13) Ojamäe, L.; Shavitt, I.; Singer, Sh. J. *J. Chem. Phys*. **1998**, *109*, 5547.
(14) Tuckerman, M.; Laasonen, K.; Sprik, M. *J. Chem. Phys*. **1995**, *103*, 150.
(15) Svanberg, M.; Pettersson, J. B. C. *J. Phys. Chem*. *A* **1998**, *102*, 1865.
(16) Kusaka, I.; Oxtoby, D. W. *J. Chem. Phys*. **2000**, *113*, 10100.
(17) Shevkunov, S. V.; Vegiri, A. *Mol. Phys.* **2000**, *98*, No 3, 149.
(18) Vegiri, A; Shevkunov, S. V. *J. Chem. Phys.* **2000**, *113*, 8521.
(19) Straatsma, T. P.; Berendsen, H. J. C.; Potsma, J. P. M. *J. Chem. Phys.* **1986**, *85*, 6720.
(20) Allen, M. P.; Tildesley, D. J. *Computer Simulation of Liquids*; Oxford University Press: Oxford, 1987.
(21) Nose, S. *Mol. Phys.* **1984**, *52*, 255
(22) Hoover, Wm, G. *Computational Statistical Mechanics*; Elsevier: New York, 1991.
(23) Kozak, R. E.; Jordan, P. C. *J. Chem. Phys*. 1993 *99*, 2978.
(24) Fornili, S. L.; Migliore, M.; Palazzo, M. A. *Chem. Phys. Lett*. **1986**, *125*, 419.
(25) Andaloro, G.; Palazzo, M. A.; Migliore, M.; Fornili, S. L. *Chem. Phys. Lett.* **1988**, *149*, 201.
(26) Khan, A. *Chem. Phys. Lett.* **2000**, *319*, 440.
(27) Kozak, R. E.; Jordan, P. C. *J. Chem. Phys*. **1992**, *96*, 3120; *ibid* 3131.
(28) Kelterbaum, R.; Kochanski, E. *J. Mol. Struct. (THEOCHEM)* **1996**, *371*, 205.
(29) Grimm, A. R. Bacskay, G. B.; Haymet, A. D. J. *Mol. Phys.* **1995**, *86*, 369.
(30) Zakharov, V. V.; Brodskaya, E. N.; Laaksonen, A. *Mol. Phys.* **1998**, *95*, 203.